RAA 2019 Vol. **19** No. **10**, 154(7pp) doi: 10.1088/1674–4527/19/10/154

http://www.raa-journal.org *http://iopscience.iop.org/raa*

Research in Astronomy and Astrophysics

Constraints on axion-like particles with different magnetic field models from the PKS 2155–304 energy spectrum

Jia Bu[1] and Ya-Ping Li[2]

[1] Department of Astronomy, Xiamen University, Xiamen 361005, China; *19820141152948@stu.xmu.edu.cn*
[2] Shanghai Astronomical Observatory, Shanghai 200030, China

Received 2018 December 19; accepted 2019 May 22

Abstract Axion-like particles (ALPs) are a promising kind of dark matter candidate particle that are predicted to couple with photons in the presence of magnetic fields. The oscillations between photons and ALPs traveling in the magnetic fields have been used to constrain ALP properties. In this work, we obtain some new constraints on the ALP mass $m_{\rm a}$ and the photon-ALP coupling constant g with two different magnetic field models through TeV photons from PKS 2155–304. The first is the discrete-φ model in which the magnetic field has the orientation angle φ that changes discretely and randomly from one coherent domain to the next, and the second is the linearly-continuous-φ model in which the magnetic field orientation angle φ varies continuously across neighboring coherent domains. For the discrete-φ model, we can obtain the best constraints on the ALP mass $m_1 = m_{\rm a}/(1\ {\rm neV}) = 0.1$ and on the photon-ALP coupling constant $g_{11} = g/(10^{-11}\ {\rm GeV}^{-1}) = 5$. The reasonable range of the ALP mass m_1 is $0.08 \sim 0.2$ when $g_{11} = 5$, and the only reasonable value of the photon-ALP coupling constant is $g_{11} = 5$ when $m_1 = 0.1$. For the linearly-continuous-φ model, we can obtain the best constraints on the ALP mass $m_1 = 0.1$ and on the photon-ALP coupling constant $g_{11} = 0.7$. The reasonable range of the ALP mass m_1 is $0.05 \sim 0.4$ when $g_{11} = 0.7$, and the reasonable range of the photon-ALP coupling constant g_{11} is $0.5 \sim 1$ when $m_1 = 0.1$. All of the results are consistent with the upper bound ($g < 6.6 \times 10^{-11}\ {\rm GeV}^{-1}$, i.e., $g_{11} < 6.6$) set by the CAST experiment.

Key words: cosmology: dark matter — gamma rays: general — galaxies: magnetic fields

1 INTRODUCTION

Axions are predicted by the Peccei-Quinn mechanism, which is a notable explanation to solve the strong charge+parity (CP) problem in quantum chromodynamics (QCD) (Peccei & Quinn 1977). In a more generic way, axion-like particles (ALPs) appear in extensions of the standard model of particle physics (Jaeckel & Ringwald 2010). In the presence of an external magnetic field $\boldsymbol{B}$, ALPs (represented by the field a) have a general property that they can couple with photons (represented by $\boldsymbol{E}$) through the interaction Lagrangian $\mathcal{L} = ga\boldsymbol{E}{\cdot}\boldsymbol{B}$. A photon can oscillate into an ALP and vice versa. These photon-ALP oscillations have been used to explain lots of astrophysical phenomena, or to constrain the properties of ALPs (Mirizzi et al. 2008). For example, the apparent dimming of supernovae (Östman & Mörtsell 2005; Mirizzi et al. 2005; Csáki et al. 2002), spectral distortions of the cosmic microwave background (Csáki et al. 2015; Dias et al. 2014) and the anomalous lack of opacity to gamma rays in the Universe. HESS, MAGIC and *Fermi* have detected high energy gamma ray photons in the TeV range from distant active galactic nuclei (AGNs) (H.E.S.S. Collaboration et al. 2013; Mazin & Raue 2007; Aharonian et al. 2006; Ackermann et al. 2012; MAGIC Collaboration et al. 2008). Before reaching the Earth, these photons will suffer significant attenuation because of electron-positron pair production on the extragalactic background infrared radiation. There is a possible interpretation for this transparency phenomenon, i.e., due to photon-ALP mixing, the radiation from AGNs travels in the form of ALPs without producing pairs during most of the distance, and converts back to photons when they arrive at Earth (Mirizzi & Montanino 2009; Burrage et al. 2009; Simet et al. 2008).

The magnetic field structure may strongly affect photon-ALP propagation in the Universe. Most of the previous studies adopted a magnetic field model in which the path of propagation is divided into many coherent domains such that each has a uniform magnetic field and the same size l. In this model, the magnetic field has an orientation angle (represented by φ) that changes discretely and randomly from one domain to the next. Based on this model, Grossman et al. (2002) derived a formula for the photon-to-ALP conversion probability through plenty of domains, and this formula has been widely used in lots of previous work. But recently, Wang & Lai (2016) adopted another magnetic field model in which the magnetic field orientation angle φ varies continuously across neighboring domains. Wang & Lai (2016) demonstrated that a qualitatively significantly different result is produced for the photon-to-ALP conversion probability compared with what is obtained in the discrete-φ model.

In this work, we compare the two different results of the photon-ALP propagation for two different magnetic field models mentioned earlier, and we obtain some new constraints on ALP properties based on photon-to-ALP conversion probability through TeV photons from a distant AGN PKS 2155–304.

This paper is organized as follows. In Section 2, we describe fitting the broadband spectral energy distribution (SED) of PKS 2155–304 with a one-zone synchrotron self-Compton (SSC) model. In Section 3, we briefly summarize the two different results of the photon-ALP propagation for the two different magnetic field models. In Section 4, we compare the constraints of ALP properties for the two different magnetic field models through fitting the survival probabilities of the TeV photons from PKS 2155–304. Our conclusions and discussion are presented in the last section.

2 OBSERVATION AND FITTING OF PKS 2155–304

Recent studies have revealed that an irregular local energy spectrum of PKS 2155–304 has been used to constrain the photon-ALP coupling (Abramowski et al. 2013). PKS 2155–304 is a powerful and well-studied TeV gamma-ray source (H.E.S.S. Collaboration et al. 2010; Aharonian et al. 2009, 2007, 2005). This BL Lac may offer the possibility for the conversion of photon-ALP in a magnetic field which lies along the path of propagation (Falomo et al. 1993; Smith et al. 1995; Abramowski et al. 2013). So, PKS 2155–304 is a good target for ALP research at high energies (Horns et al. 2012).

Table 1 The One-Zone SSC Model Parameters for PKS 2155–304

δ	B (G)	R (cm)	N_0 (cm^{-3})	$\gamma_{\min}$	γ_0	$\gamma_{\max}$	p_1	p_2
35	1.2	8×10^{15}	6000	1100	9000	10^7	2	4.54

δ is the Doppler factor, B is the uniform magnetic field, R is the radius of the emitting blob, N_0 is the density factor, $\gamma_{\min}$, γ_0 and $\gamma_{\max}$ are the minimum, break and maximum Lorentz factors of the electron energy distribution respectively, and p_1 and p_2 are the spectral indexes of the electron energy distribution at lower and higher energies respectively.

We have collected the broadband observed data from the NASA/IPAC Extragalactic Database (NED), along with TeV data from the HESS observations. We fit the broadband SED of PKS 2155–304 with a one-zone SSC model developed by Chen (2017). In this one-zone SSC model, there are nine independent parameters that describe the broadband SED. Three parameters characterize the global properties of the emitting blob: δ, the Doppler factor, B, the uniform magnetic field and R, the radius of the emitting blob. The other six parameters characterize the distribution and physical properties of the high-energy particles: p_1 and p_2, the spectral indexes of the electron energy distribution at lower and higher energies respectively, $\gamma_{\max}$, $\gamma_{\min}$ andγ_0, the maximum, minimum and break Lorentz factors of the electron energy distribution respectively, and N_0, the density factor. In this model, the synchrotron + SSC emissions can produce the whole SED. We can adjust the nine free independent parameters as mentioned above to fit the SED of PKS 2155–304. Figure 1 presents our fitting, and the corresponding parameters are listed in Table 1. In Figure 1, the red line indicates the one-zone SSC fitting of the SED of PKS 2155–304, the black open squares represent the broadband observation data from NED and the black filled circles signify TeV data from the HESS observations (Aharonian et al. 2005).

We briefly summarize the two different results of the photon-ALP propagation for two different models of the magnetic field along the path of propagation, and we refer interested readers to Kuo & Pantaleone (1989), Grossman et al. (2002) and Wang & Lai (2016) for further details.

3 PHOTON-ALP PROPAGATION FOR TWO MAGNETIC FIELD MODELS

In Cartesian XYZ coordinates (the Z-axis is along the direction of propagation), if the angular frequency ω or energy ε is given (for $\boldsymbol{E}$, $a \propto e^{i\omega t}$), then the evolution equa-

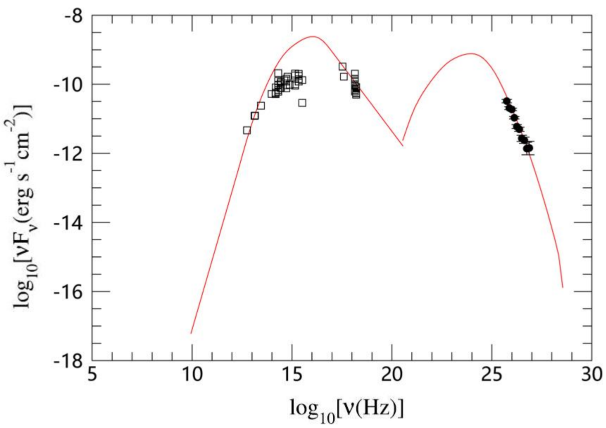

Fig. 1 The fitting of the broadband SED of PKS 2155–304, where the *red line* indicates the one-zone SSC fitting of the SED of PKS 2155–304, the *black open squares* represent the broadband observed data from NED and the *black filled circles* signify TeV data from the HESS observations (Aharonian et al. 2005) (*Color version is online*).

tion of ALP field a and the photon electric field $\boldsymbol{E}$ can take the form

$$i\begin{pmatrix} a' \\ E'_x \\ E'_y \end{pmatrix} = \begin{pmatrix} \omega+\Delta_\mathrm{a} & \Delta_\mathrm{M}\cos\varphi & \Delta_\mathrm{M}\sin\varphi \\ \Delta_\mathrm{M}\cos\varphi & \omega+\Delta_\mathrm{pl} & 0 \\ \Delta_\mathrm{M}\sin\varphi & 0 & \omega+\Delta_\mathrm{pl} \end{pmatrix}\begin{pmatrix} a \\ E_x \\ E_y \end{pmatrix}, \tag{1}$$

where the superscript $'$ represents d/dz and φ is the orientation angle of the magnetic field $\boldsymbol{B}$, i.e., φ is the angle between $\boldsymbol{B}_\mathrm{tr}$ (the projection of $\boldsymbol{B}$ in the XY-plane) and the X-axis. If we define dimensionless quantities (in units of $c = \hbar = 1$),

$$\begin{aligned} m_1 &= m_\mathrm{a}/(1\ \mathrm{neV}), \\ \varepsilon_1 &= \varepsilon/(1\ \mathrm{TeV}), \\ g_{11} &= g/(10^{-11}\ \mathrm{GeV}^{-1}), \\ B_1 &= B_\mathrm{tr}/(1\ \mathrm{nG}). \end{aligned} \tag{2}$$

The parameter Δ_a is related to the ALP mass and the parameter Δ_M is related to the photon-ALP coupling constant, which are given by

$$\Delta_\mathrm{a} = -\frac{m_\mathrm{a}^2}{2\omega} = -7.83\times10^{-2}\varepsilon_1^{-1}m_1^2\,\mathrm{Mpc}^{-1}, \tag{3}$$

and

$$\Delta_\mathrm{M} = \frac{1}{2}gB_\mathrm{tr} = 4.63\times10^{-3}g_{11}B_1\,\mathrm{Mpc}^{-1}, \tag{4}$$

where m_a is the ALP mass, ε is the photon energy and g is the photon-ALP coupling constant. The plasma parameter $\Delta_\mathrm{pl} = -\omega_\mathrm{pl}^2/(2\omega) = -1.11\times 10^{-11}\varepsilon_1^{-1}(n_\mathrm{e}/10^{-7}\ \mathrm{cm}^{-3})\,\mathrm{Mpc}^{-1}$, where ω_pl is the electron plasma frequency and n_e is the electron density.

The photon-ALP evolution can be obtained by integrating Equation (10) along the ray for a given magnetic field structure. We assume that the path of propagation is divided into many coherent domains, and each has a uniform magnetic field and the same size l.

For the model in which the magnetic field has an orientation angle φ and changes discretely and randomly from one domain to the next, Grossman et al. (2002) derived an analytic formula for the mean value of the photon-to-ALP conversion probability (represented by P_G) after propagating through N domains (over distance $D = Nl$). This formula has been widely used in a number of previous studies

$$P_\mathrm{G} = \frac{1}{3}(1 - e^{-3NP_0/2}), \tag{5}$$

where

$$P_0 = \frac{\Delta_\mathrm{M}^2}{(\Delta k/2)^2}\sin^2(\Delta kD/2), \tag{6}$$

and $\Delta k = \sqrt{\Delta_\mathrm{a}^2 + 4\Delta_\mathrm{M}^2}$.

For the model in which the magnetic field orientation angle φ varies linear-continuously across neighboring domains, Wang & Lai (2016) obtained a numerical result indicating that this continuous-φ model can generate completely different photon-to-ALP conversion probability compared to the discrete-φ model. The mean photon-to-ALP conversion probability (represented by P_W) after propagating through N domains (over distance $D = Nl$) is

$$P_\mathrm{W} \simeq 0.123\frac{\Delta_\mathrm{M}^2}{\Delta_\mathrm{a}^2}[1-\cos(N\Delta_\mathrm{a}l)] + \sigma_\mathrm{A}^2 N\Delta_\mathrm{M}^2 l^2. \tag{7}$$

It is notable that the validity of Equation (7) requires $P_\mathrm{W} \ll 1$ (Wang & Lai 2016).

4 CONSTRAINTS ON ALP PROPERTIES

Based on the fitting of the broadband SED of PKS 2155–304 (see Fig. 1), we can calculate the survival probabilities (represented by P_S) of the TeV photons from PKS 2155–304: $P_\mathrm{S} = F_\mathrm{obs}/F_\mathrm{source}$, where F_obs is the observed fluxes of TeV photons and F_source is the fluxes of the TeV photons before propagation in the Universe, i.e., the fitting values of the SED for PKS 2155–304.

We can also derive the TeV photon survival probabilities through the photon-to-ALP conversion probabilities because the survival probability plus the conversion probability equals 1 for a single photon.

For the model in which the magnetic field has the orientation angle φ changing discretely and randomly from one domain to the next, the TeV photon survival probability (represented by $P_{\mathrm{S,G}}$) is

$$P_{\mathrm{S,G}} = 1 - P_{\mathrm{G}} = \frac{2}{3} + \frac{1}{3}e^{-3NP_0/2}. \tag{8}$$

For the model in which the magnetic field orientation angle φ varies linear-continuously across neighboring domains, the TeV photon survival probability (represented by $P_{\mathrm{S,W}}$) is

$$\begin{aligned} P_{\mathrm{S,W}} &= 1 - P_{\mathrm{W}} \\ &\simeq 1 - 0.123\frac{\Delta_{\mathrm{M}}^2}{\Delta_{\mathrm{a}}^2}[1-\cos(N\Delta_{\mathrm{a}}l)] - \sigma_{\mathrm{A}}^2 N\Delta_{\mathrm{M}}^2 l^2. \end{aligned} \tag{9}$$

Note that the magnetic field structure around the source and in the intergalactic medium (IGM) are very different. Typically, the intergalactic magnetic field has an upper limit of a few nG and the coherent domain size is on the order of a few Mpc, but the strength of the magnetic field around the source is about $0.1 \sim 1$ G and coherent domain size is about $0.1 \sim$ a few pc (Sánchez-Conde et al. 2009; Grasso & Rubinstein 2001; Grossman et al. 2002; Ade et al. 2015). For PKS 2155–304, in our calculation, we adopt the following scheme: the strength of the magnetic field around the source (represented by B_{sou}) we apply is about 1.2 G, which is the value employed in our SSC model (see Table 1), and the coherent domain size around the source (represented by l_{sou}) we utilize is about $1\,\mathrm{pc}$, which is the distance from the central black hole to the broad line region (BLR); the strength of the intergalactic magnetic field (represented by B_{int}) we implement is about $1\,\mathrm{nG}$, and the intergalactic coherent domain size (represented by l_{int}) we use is about $1\,\mathrm{Mpc}$. We have listed all these values in Table 2.

If the survival probability of a TeV photon that propagates through the magnetic field around the source is represented by $P_{\mathrm{S,sou}}$, and the survival probability of propagating through the intergalactic magnetic field is represented by $P_{\mathrm{S,int}}$, the total survival probability can be written as

$$P_{\mathrm{S}} = P_{\mathrm{S,sou}} \times P_{\mathrm{S,int}}. \tag{10}$$

It is notable that the generated ALPs in the magnetic field around the source would be partially converted back to photons in the intergalactic magnetic field. However, based on our calculations, we find that this effect is too small for the total survival probability, so we can neglect it.

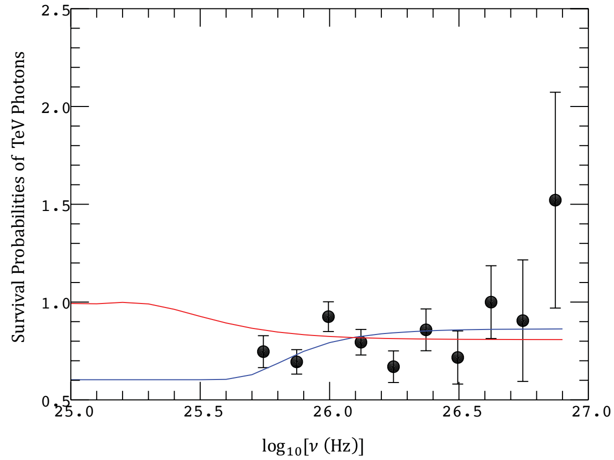

Fig. 2 The best fitting of survival probabilities for the TeV photons from PKS 2155–304 for the two different models. Here the *black filled circles* represent the survival probabilities (P_{S}) of all the TeV photons. The *blue line* indicates the best fitting for the discrete-φ model ($P_{\mathrm{S,G}}$), and the corresponding parameter values are: $m_1 = 0.1$ and $g_{11} = 5$. The *red line* marks the best fitting for the linearly-continuous-φ model ($P_{\mathrm{S,W}}$), and the corresponding parameter values are: $m_1 = 0.1$ and $g_{11} = 0.7$. The *highest black filled circle* is not considered in our fitting, because its error is too big and the survival probability it represents is greater than one, which is unphysical.

For the two different models, we have

$$\begin{aligned} P_{\mathrm{S,G}} =& P_{\mathrm{S,G,sou}} \times P_{\mathrm{S,G,int}} \\ =& \left(\frac{2}{3} + \frac{1}{3}e^{-3NP_0/2}\right)_{\mathrm{sou}} \\ & \times \left(\frac{2}{3} + \frac{1}{3}e^{-3NP_0/2}\right)_{\mathrm{int}}, \end{aligned} \tag{11}$$

and

$$\begin{aligned} P_{\mathrm{S,W}} =& P_{\mathrm{S,W,sou}} \times P_{\mathrm{S,W,int}} \\ =& \Big(1 - 0.123\frac{\Delta_{\mathrm{M}}^2}{\Delta_{\mathrm{a}}^2}\left[1-\cos(N\Delta_{\mathrm{a}}l)\right] \\ & - \sigma_{\mathrm{A}}^2 N\Delta_{\mathrm{M}}^2 l^2\Big)_{\mathrm{sou}} \times \Big(1 - 0.123\frac{\Delta_{\mathrm{M}}^2}{\Delta_{\mathrm{a}}^2} \\ & \times [1-\cos(N\Delta_{\mathrm{a}}l)] - \sigma_{\mathrm{A}}^2 N\Delta_{\mathrm{M}}^2 l^2\Big)_{\mathrm{int}}. \end{aligned} \tag{12}$$

In Equations (11) and (12), we can adjust the parameters m_1 and g_{11} to make a best fitting of the survival probabilities for the TeV photons from PKS 2155–304.

In Figure 2, we present the survival probabilities (P_{S}) of all the TeV photons, which are represented by black filled circles. We also present the best fitting curves for the discrete-φ model ($P_{\mathrm{S,G}}$) and for the linearly-continuous-φ model ($P_{\mathrm{S,W}}$). In Equation (11), when the ALP mass $m_1 = 0.1$ and the photon-ALP coupling constant $g_{11} = 5$, we can obtain the best fitting curve of $P_{\mathrm{S,G}}$, which is indicated by the blue line. For Equation (12), when $m_1 = 0.1$

Table 2 Parameters Used to Calculate the Total Photon-axion Conversion Both in the Magnetic Field around the Source and in the Intergalactic Magnetic Field

	Parameter	Discrete-φ model	Linearly-continuous-φ model
Source parameters	$B_{\rm sou}$	1.2 G	1.2 G
	$l_{\rm sou}$	1 pc	1 pc
Intergalactic parameters	$B_{\rm int}$	1 nG	1 nG
	$l_{\rm int}$	1 Mpc	1 Mpc
ALP parameters (best fitting)	$m_{\rm a}$	0.1 neV	0.1 neV
	g	5×10^{-11} GeV^{-1}	0.7×10^{-11} GeV^{-1}

$B_{\rm sou}$ represents the strength of the magnetic field around the source, $l_{\rm sou}$ indicates the coherent domain size around the source, $B_{\rm int}$ signifies the strength of the intergalactic magnetic field, $l_{\rm int}$ corresponds to the intergalactic coherent domain size, $m_{\rm a}$ tells the ALP mass and g denotes the photon-ALP coupling constant.

and $g_{11} = 0.7$, we can obtain the best fitting curve of $P_{\rm S,W}$, which is marked by the red line. It is notable that we did not consider the highest black filled circle in Figure 2 in our fitting because its error is too big and the survival probability it represents is greater than one, which is unphysical.

For the discrete-φ model, we present a few typical fitting curves in Figure 3. The left panel displays the different fitting curves of $P_{\rm S,G}$ with different m_1 when $g_{11} = 5$: the blue line represents $m_1 = 0.08$, the red line indicates $m_1 = 0.1$ and the black line signifies $m_1 = 0.2$. So, the reasonable range of the ALP mass m_1 is 0.08 $\sim$ 0.2 when $g_{11} = 5$. The right panel depicts the different fitting curves of $P_{\rm S,G}$ with different g_{11} when $m_1 = 0.1$: the red line marks $g_{11} = 5$, the black line traces $g_{11} = 10$ and the blue line shows that g_{11} takes other values. So, the only reasonable value of the photon-ALP coupling constant is $g_{11} = 5$ when $m_1 = 0.1$. These results imply that, in the energy range $10^{25} - 10^{27}$ Hz, for the discrete-φ model, the TeV photon survival probabilities $P_{\rm S,G}$ are very sensitive to the ALP mass m_1, but are not sensitive to the photon-ALP coupling constant g_{11}.

For the linearly-continuous-φ model, we also present a few typical fitting curves in Figure 4. The left panel shows the different fitting curves of $P_{\rm S,W}$ with different m_1 when $g_{11} = 0.7$: the blue line represents $m_1 = 0.05$, the red line signifies $m_1 = 0.1$, the black line indicates $m_1 = 0.2$ and the green line corresponds to $m_1 = 0.4$. So, the reasonable range of the ALP mass m_1 is 0.05 $\sim$ 0.4 when $g_{11} = 0.7$. The right panel depicts the different fitting curves of $P_{\rm S,W}$ with different g_{11} when $m_1 = 0.1$: the black line represents $g_{11} = 0.5$, the red line signifies $g_{11} = 0.7$, the blue line indicates $g_{11} = 0.8$ and the green line traces $g_{11} = 1$. So, the reasonable range of the photon-ALP coupling constant g_{11} is 0.5 $\sim$ 1 when $m_1 = 0.1$. These results imply that, in the energy range 10^{25} Hz-10^{27} Hz, for the linearly-continuous-φ model, the TeV photon survival probabilities $P_{\rm S,W}$ are very sensitive to the ALP mass m_1, and are also very sensitive to the photon-ALP coupling constant g_{11}.

It is difficult to explain why there is only one reasonable value of the photon-ALP coupling constant (i.e., $g_{11} = 5$) when $m_1 = 0.1$ for the discrete-φ model, but for the two models, the best-fitting parameters of ALPs and the reasonable ranges of the parameters of ALPs which are based on the best fitting are consistent with the upper bound ($g < 6.6 \times 10^{-11}$ GeV^{-1}, i.e., $g_{11} < 6.6$) set by the CAST experiment (Anastassopoulos et al. 2017). Comparing the fitting results of the two different models, we can find that the best-fitting g_{11} which comes from the linearly-continuous-φ model ($g_{11} = 0.7$) is almost one order of magnitude smaller than the one that comes from the discrete-φ model ($g_{11} = 5$). This means that the coupling between photon and ALP in the linearly-continuous-φ magnetic field structure is much weaker than in the discrete-φ magnetic field structure, but the physical mechanism involved is still unclear.

5 SUMMARY AND DISCUSSION

ALPs are a promising kind of dark matter candidate particle that are predicted to couple with photons in the presence of magnetic fields. An ALP can oscillate into a photon and vice versa due to this coupling process. Such photon-ALP oscillations have been used to interpret observations of TeV gamma-ray photons from extragalactic sources, which are unexpected due to the electron-positron pair production process. In this paper, we obtain some new constraints on ALP properties based on photon-to-ALP conversion probability through TeV photons detected from a distant AGN PKS 2155–304.

First, we fit the broadband SED of PKS 2155–304 with a one-zone SSC model. Based on the fitting of its broadband SED, we can obtain the strength of the magnetic field $B = 1.2$ G around PKS 2155–304, and the survival probabilities of these TeV photons. By making fur-

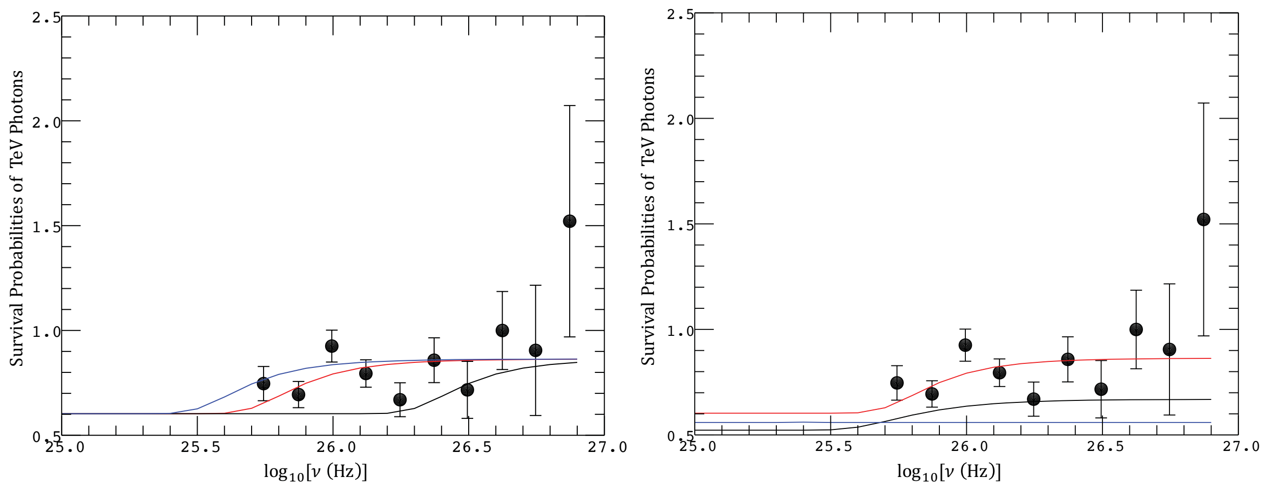

Fig. 3 A few typical fitting curves for the discrete-φ model. The left panel displays the different fitting curves of $P_{\rm S,G}$ with different m_1 when $g_{11} = 5$: the *blue line* represents $m_1 = 0.08$, the *red line* indicates $m_1 = 0.1$ and the *black line* signifies $m_1 = 0.2$. The right panel depicts the different fitting curves of $P_{\rm S,G}$ with different g_{11} when $m_1 = 0.1$: the *red line* marks $g_{11} = 5$, the *black line* traces $g_{11} = 10$ and the *blue line* shows that g_{11} takes other values.

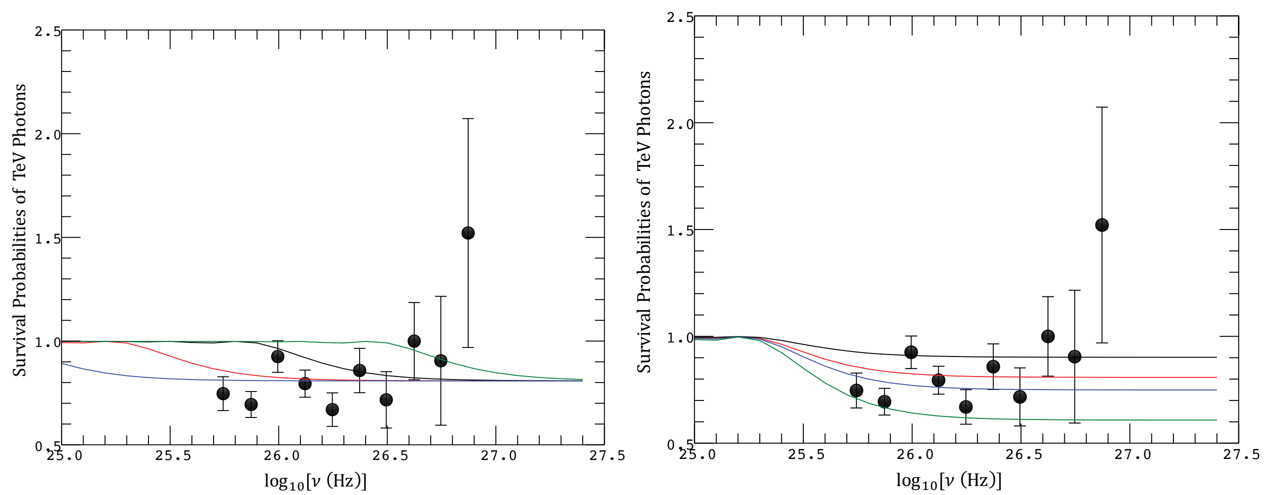

Fig. 4 A few typical fitting curves for the linearly-continuous-φ model. The left panel shows the different fitting curves of $P_{\rm S,W}$ with different m_1 when $g_{11} = 0.7$: the *blue line* represents $m_1 = 0.05$, the *red line* signifies $m_1 = 0.1$, the *black line* indicates $m_1 = 0.2$ and the *green line* corresponds to $m_1 = 0.4$. The right panel depicts the different fitting curves of $P_{\rm S,W}$ with different g_{11} when $m_1 = 0.1$: the *black line* represents $g_{11} = 0.5$, the *red line* signifies $g_{11} = 0.7$, the *blue line* indicates $g_{11} = 0.8$ and the *green line* traces $g_{11} = 1$.

ther reasonable assumptions that the coherent domain size around the source is the distance from the central black hole to BLR (e.g., 1 pc), and about the strength of the intergalactic magnetic field (e.g., 1 nG) and the intergalactic coherent domain size (e.g., 1 Mpc), we can constrain the two key parameters for ALP, i.e., the particle mass m_a and the photon-ALP coupling constant g based on the survival probability of TeV photons. Two magnetic field configurations are considered based on the previous studies. One is the discrete-φ model. In this model, the path of propagation is divided into lots of coherent domains such that each has a uniform magnetic field and the same size l, and the magnetic field has the orientation angle φ changing discretely and randomly from one domain to the next. Another is the linearly-continuous-φ model in which the magnetic field orientation angle φ varies continuously across neighboring domains.

For the discrete-φ model, when $m_1 = 0.1$ and $g_{11} = 5$ ($m_1 \equiv m_{\rm a}/1$ neV, and $g_{11} \equiv g/10^{-11}$ GeV^{-1}), we can obtain the best fitting curve of $P_{\rm S,G}$. The reasonable range of the ALP mass m_1 is $0.08 \sim 0.2$ when $g_{11} = 5$, and the only reasonable value of the photon-ALP coupling constant is $g_{11} = 5$ when $m_1 = 0.1$. These results imply that, in the energy range $10^{25} - 10^{27}$ Hz, for the discrete-φ

model, the TeV photon survival probabilities $P_{\mathrm{S,G}}$ are very sensitive to the ALP mass m_1, but are not sensitive to the photon-ALP coupling constant g_{11}.

For the linearly-continuous-φ model, when $m_1 = 0.1$ and $g_{11} = 0.7$, we can obtain the best fitting curve of $P_{\mathrm{S,W}}$. The reasonable range of the ALP mass m_1 is 0.05 $\sim$ 0.4 when $g_{11} = 0.7$, and the reasonable range of the photon-ALP coupling constant g_{11} is 0.5 ~ 1 when $m_1 = 0.1$. These results imply that, in the energy range $10^{25} - 10^{27}$ Hz, for the linearly-continuous-φ model, the TeV photon survival probabilities $P_{\mathrm{S,W}}$ are very sensitive to the ALP mass m_1, and are also very sensitive to the photon-ALP coupling constant g_{11}.

It is notable that, for the two models, the best-fitting parameters of ALPs and the reasonable ranges of the parameters of ALPs which are based on the best fitting are consistent with the upper bound ($g < 6.6 \times 10^{-11}\,\mathrm{GeV}^{-1}$, i.e., $g_{11} < 6.6$) set by the CAST experiment. Comparing the fitting results of the two different models, we can find that the best-fitting g_{11} which comes from the linearly-continuous-φ model ($g_{11} = 0.7$) is almost one order of magnitude smaller than the one that comes from the discrete-φ model ($g_{11} = 5$). This means that the coupling between photon and ALP in the linearly-continuous-φ magnetic field structure is much weaker than in the discrete-φ magnetic field structure, but the physical mechanism involved is still unclear.

Although PKS 2155–304 is a well-studied TeV gamma-ray emitter, the TeV observations we can acquire are still limited. More publicly available TeV observations of PKS 2155–304 are necessary to obtain more precise constraints on ALP properties.

Acknowledgements We thank Dr. Feng Huang for useful discussions and comments, which helped to improve the manuscript.

References

Anastassopoulos, V., Aune, S., Barth, K., et al. 2017, Nature Physics, 13, 584
Ade, P. A. R., Arnold, K., Atlas, M., et al. 2015, Phys. Rev. D, 92, 123509
Abramowski, A., Acero, F., Aharonian, F., et al. 2013, Phys. Rev. D, 88, 102003
Aharonian, F., Akhperjanian, A. G., Bazer-Bachi, A. R., et al. 2005, A&A, 442, 895
Aharonian, F., Akhperjanian, A. G., Aye, K.-M., et al. 2005, A&A, 430, 865
Aharonian, F., Akhperjanian, A. G., Bazer-Bachi, A. R., et al. 2007, ApJ, 664, L71
Aharonian, F., Akhperjanian, A. G., Anton, G., et al. 2009, ApJ, 696, L150
Ackermann, M., Ajello, M., Allafort, A., et al. 2012, Science, 338, 1190
Aharonian, F., Akhperjanian, A. G., Bazer-Bachi, A. R., et al. 2006, Nature, 440, 1018
Burrage, C., Davis, A.-C., & Shaw, D. J. 2009, Physical Review Letters, 102, 201101
Csáki, C., Kaloper, N., & Terning, J. 2002, Physical Review Letters, 88, 161302
Csáki, C., Kaloper, N., & Terning, J. 2015, J. Cosmol. Astropart. Phys., 6, 041
Chen, L. 2017, ApJ, 842, 129
Dias, A. G., Machado, A. C. B., Nishi, C. C., Ringwald, A., & Vaudrevange, P. 2014, Journal of High Energy Physics, 6, 37
Falomo, R., Pesce, J. E., & Treves, A. 1993, ApJ, 411, L63
Grossman, Y., Roy, S., & Zupan, J. 2002, Physics Letters B, 543, 23
Grasso, D., & Rubinstein, H. R. 2001, Phys. Rep., 348, 163
Horns, D., Maccione, L., Meyer, M., et al. 2012, Phys. Rev. D, 86, 075024
H.E.S.S. Collaboration, Abramowski, A., Acero, F., et al. 2013, A&A, 550, A4
H.E.S.S. Collaboration, Abramowski, A., Acero, F., et al. 2010, A&A, 520, A83
Jaeckel, J., & Ringwald, A. 2010, Annual Review of Nuclear and Particle Science, 60, 405
Kuo, T. K., & Pantaleone, J. 1989, Reviews of Modern Physics, 61, 937
Mirizzi, A., Raffelt1, G. G., & Serpico, P. D. 2008, Axions, 741, 115
Mirizzi, A., Raffelt, G. G., & Serpico, P. D. 2005, Phys. Rev. D, 72, 023501
Mirizzi, A., & Montanino, D. 2009, J. Cosmol. Astropart. Phys., 12, 004
Mazin, D., & Raue, M. 2007, A&A, 471, 439
MAGIC Collaboration, Albert, J., Aliu, E., et al. 2008, Science, 320, 1752
Östman, L., & Mörtsell, E. 2005, J. Cosmol. Astropart. Phys., 2, 005
Peccei, R. D., & Quinn, H. R. 1977, Physical Review Letters, 38, 1440
Simet, M., Hooper, D., & Serpico, P. D. 2008, Phys. Rev. D, 77, 063001
Smith, E. P., O'Dea, C. P., & Baum, S. A. 1995, ApJ, 441, 113
Sánchez-Conde, M. A., Paneque, D., Bloom, E., Prada, F., & Domínguez, A. 2009, Phys. Rev. D, 79, 123511
Wang, C., & Lai, D. 2016, J. Cosmol. Astropart. Phys., 6, 006